

Ambipolar Polymer Field-Effect Transistors Based on Fluorinated Isoindigo: High Performance and Improved Ambient Stability

Ting Lei,[†] Jin-Hu Dou,[†] Zhi-Jun Ma,[‡] Cong-Hui Yao,[†] Chen-Jiang Liu,^{*,‡} Jie-Yu Wang,[†] and Jian Pei^{*,†}

[†]Beijing National Laboratory for Molecular Sciences, the Key Laboratory of Bioorganic Chemistry and Molecular Engineering of Ministry of Education, College of Chemistry and Molecular Engineering, Peking University, Beijing 100871, China

[‡]Physics and Chemistry Detecting Center, the Key Laboratory of Oil & Gas Fine Chemicals of Ministry of Education, School of Chemistry and Chemical Engineering, Xinjiang University, Urumqi 830046, China

Supporting Information

ABSTRACT: Ambipolar transport behavior in isoindigo-based conjugated polymers is observed for the first time. Fluorination on the isoindigo unit effectively lowers the LUMO level of the polymer and significantly increases the electron mobility from 10^{-2} to $0.43 \text{ cm}^2 \text{ V}^{-1} \text{ s}^{-1}$ while maintaining high hole mobility up to $1.85 \text{ cm}^2 \text{ V}^{-1} \text{ s}^{-1}$ for FET devices fabricated in ambient. Further investigation indicates that fluorination also affects the interchain interactions of polymer backbones, thus leading to different polymer packing in thin films.

Ambipolar polymer field-effect transistors (FETs), capable of both hole and electron transport, exhibit simpler processing requirements in complementary-like circuits and potential application in organic light-emitting transistors.^{1–3} Recently, diketopyrrolopyrrole (DPP) based ambipolar polymer FETs have shown remarkable hole and electron mobilities (over $1 \text{ cm}^2 \text{ V}^{-1} \text{ s}^{-1}$).^{3,4} However, high hole/electron mobilities based on these devices were achieved under nitrogen. Further investigation on ambipolar polymers which operate in ambient is very important for their practical applications,^{3,4} as well as fundamental understanding of the carrier transport in conjugated polymers.⁵

Isoindigo has been used as the acceptor unit to construct low band gap donor-acceptor copolymers for organic photovoltaics (OPVs) and *p*-type FETs.^{6–8} The highly electron deficient isoindigo unit endows these copolymers with intriguing properties, such as broad absorption and high open circuit voltage in OPVs,⁶ as well as high hole mobility and good ambient stability in FETs.^{7,8} Nevertheless, isoindigo-based polymers have extremely low electron mobility (the highest one is only $3.7 \times 10^{-7} \text{ cm}^2 \text{ V}^{-1} \text{ s}^{-1}$),⁹ albeit their low-lying LUMO levels (-3.6 to -3.8 eV),^{6–9} thus limiting their application in *n*-type FETs¹⁰ or as acceptors in OPVs.¹¹

Herein, we introduce fluorine atoms onto the isoindigo units of the polymer to further lower its LUMO level, intending to improve the electron mobility of isoindigo-based polymer FETs. Fluorination of the backbone of polymers can effectively improve the performance of OPVs, because fluorine is electron-withdrawing and small, hence capable of modulating the electronic properties of polymers without deleterious steric effects.¹² To our delight, fluorinated isoindigo-based polymer FETs fabricated in ambient show electron mobility up to $0.43 \text{ cm}^2 \text{ V}^{-1} \text{ s}^{-1}$, while maintaining hole mobility up to $1.85 \text{ cm}^2 \text{ V}^{-1}$

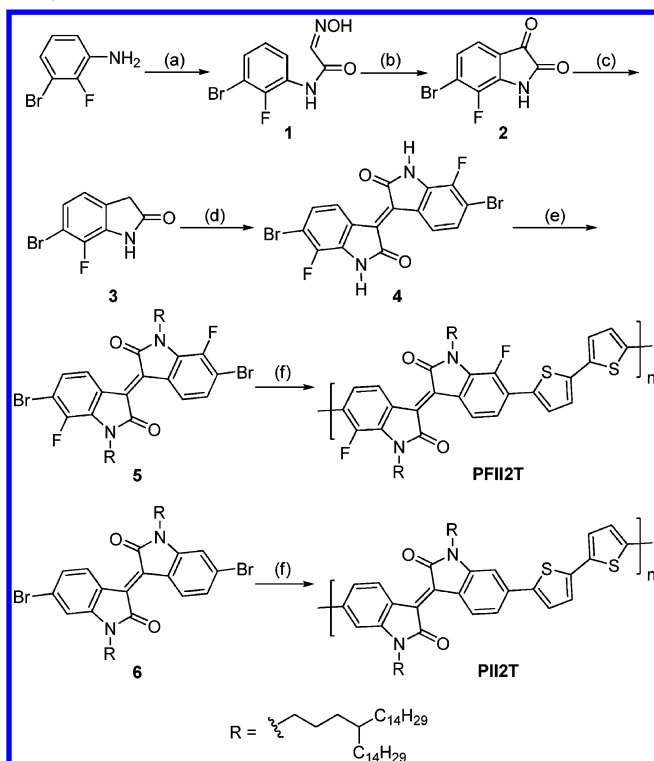
s^{-1} . This represents the first ambipolar transport behavior for isoindigo-based polymers. To the best of our knowledge, these mobilities are the highest for an ambipolar FET fabricated under ambient conditions.¹³

Recently, we demonstrated that modulating branched alkyl chains in isoindigo-based polymers significantly increased the hole mobility.^{7a} The 4-tetradecyloctadecyl group was chosen as the side chain of the fluorinated polymer. Scheme 1 shows the synthetic route to polymers **PFI2T** and **PII2T**. Commercially available 3-bromo-2-fluoroaniline was condensed with chloral hydrate and hydroxylamine hydrochloride to afford compound **1**, catalyzed by sulfuric acid. In presence of conc. sulfuric acid, crude **1** underwent cyclization to provide 6-bromo-7-fluoroisatin (**2**) in 61% yield. A two-step Wolff-Kishner-Huang reduction was used to reduce the carbonyl group to methylene, giving **3**. Direct condensation of **2** and **3** in acetic acid afforded 6,6'-difluoroisoindigo (**4**) in 72% yield. Initial attempts to alkylate **4** with 15-(3-iodopropyl)nonacosane using K_2CO_3 failed, presumably due to the steric hindrance caused by fluorines. A stronger base KOH was then used, and the reaction proceeded smoothly at room temperature to give **5** in 88% yield. A Stille coupling polymerization between **5** and 5,5'-bis-(trimethylstannyl)-2,2'-bithiophene gave polymer **PFI2T** in high yield. **PII2T** was prepared as a reference polymer to study the effect of fluorination. Both polymers were purified by adding a coordinating ligand to remove residual palladium catalyst, then Soxhlet extraction to remove oligomers and other impurities. Molecular weight of both polymers was evaluated by high temperature gel permeation chromatography (GPC) with 1,2,4-trichlorobenzene (TCB) as eluent at $140 \text{ }^\circ\text{C}$. Both polymers show comparable M_n (**PFI2T**, 75.7 kDa; **PII2T**, 72.8 kDa). Nonetheless, the PDI of **PFI2T** (2.58) is larger than that of **PII2T** (1.95). Both polymers show excellent thermal stability with decomposition temperature over $410 \text{ }^\circ\text{C}$. No phase transition was observed for both polymers by differential scanning calorimetry in the range of room temperature to $330 \text{ }^\circ\text{C}$.

Figure 1a illustrates the absorption spectra of both polymers in dilute solution and in thin film. Both polymers show typically dual absorption bands. After introducing fluorine atoms, the charge transfer absorption band (Band I) of **PFI2T** red-shifts obviously, whereas the Band II blue-shifts slightly and the

Received: October 17, 2012

Published: November 29, 2012

Scheme 1. Synthesis of Fluorinated Isoindigo-Based Polymers^a

^aReagents and conditions: (a) $\text{NH}_2\text{OH}\cdot\text{HCl}$, $\text{CCl}_3\text{CH}(\text{OH})_2$, H_2SO_4 (aq.), 130 °C; (b) conc. H_2SO_4 , 70 °C, 61% for 2 steps; (c) (i) $\text{N}_2\text{H}_4\cdot\text{H}_2\text{O}$ (85%), EtOH, reflux; (ii) *t*-BuONa, EtOH, reflux, 56%; (d) 2, AcOH/HCl, reflux, 24 h, 72%; (e) 15-(3-iodopropyl)nonacosane, powder KOH, DMSO/THF (1:1), 20 °C, 88%; (f) 5,5'-bis-(trimethylstannyl)-2,2'-bithiophene, Pd_2dba_3 , P(*o*-tol)₃, toluene, 110 °C, 48 h, for PFI2T, 99%; for PII2T, 94%.

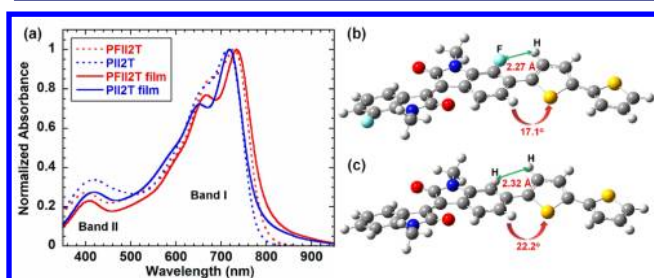


Figure 1. (a) Normalized UV-vis absorption spectra of both polymers in CHCl_3 (1×10^{-5} M) and in thin film. Molecular models of (b) PFI2T and (c) PII2T fragments. Alkyl chains were replaced by methyl groups for simplicity (geometries were optimized at B3LYP/6-31G(d) level). PFI2T displays smaller dihedral angle (17.1°) and shorter F–H distance (2.27 Å).

absorption intensity is decreased. Compared with those in solution, absorption spectra of both polymers in thin film show a slight red-shift and increased *0–0* vibrational absorption, indicating that the polymer backbones become more planar in the solid state. The bandgap of PFI2T in thin film estimated from the absorption onset is 1.50 eV, 0.07 eV smaller than that of PII2T. Interestingly, computational analysis of the fragment structure reveals that the introduction of fluorine atoms does not increase the dihedral angle of polymer backbones. Instead, because of fluorine/hydrogen interaction, the phenyl-thienyl

rotational angle of the fluorinated monomer is decreased from 22.2° to 17.1°, and the calculated F–H distance (2.27 Å) is significantly shorter than the sum of the F–H van der Waals radii (2.56 Å)¹⁴ (Figure 1b,c). This result indicates that the introduction of fluorine atoms provides the polymer with a planar backbone, which is consistent with the absorption features.

Electrochemical properties of both polymers are explored by cyclic voltammetry (CV) measurement. Both polymers show much stronger oxidative peaks than their reductive ones (Figure 2a). After introducing fluorine atoms, the reduction current of

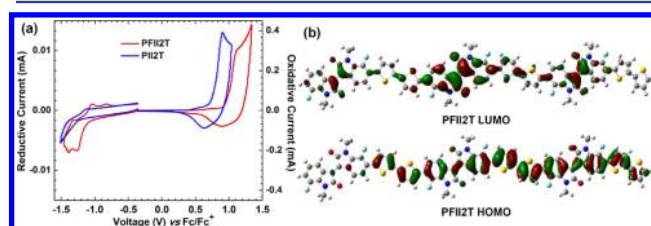


Figure 2. (a) Cyclic voltammograms of both polymers in thin film drop-cast on a glassy carbon electrode. (b) Calculated molecular orbitals of the trimer of PFI2T (B3LYP/6-31G(d)).

PFI2T increased and the doping processes appeared to be more reversible than those of PII2T. Compared with those of PII2T, both HOMO and LUMO levels of PFI2T are obviously decreased. The LUMO level of PFI2T measured by CV reaches -3.88 eV, 0.18 eV lower than that of PII2T. In our previous report, changing the donor part of isoindigo-based polymers hardly affects the LUMO levels of polymers,^{8a} because their LUMO levels are mostly localized on isoindigo cores (Figure 2b). Herein, fluorination of isoindigo core effectively lowers the LUMO level. The HOMO level is also lowered after the fluorination, because the HOMOs of polymers are well delocalized along the backbone. The CV results are consistent with the photoelectron spectroscopy (PES) measurement. The optical bandgaps and PES results give HOMO/LUMO levels of $-5.46/-3.96$ eV for PFI2T and $-5.31/-3.74$ eV for PII2T. Photophysical and electrochemical properties of both polymers are in Table S1. Note that the low-lying LUMO level of PFI2T is lower than several ambient-stable ambipolar polymers¹³ and even comparable to some air-stable n-type polymers based on perylenedicarboximide (PDI) and naphthalenedicarboximide (NDI).^{10a} Hence, ambient-stable charge transport in PFI2T is expected.

To test the ambipolar transport capability of our isoindigo-based polymers, a top-gate/bottom-contact (TG/BC) device structure was used to fabricate polymer FETs. This device configuration is preferred for ambient-stable ambipolar or n-type organic materials, because of its better injection characteristics and the encapsulation effect of the top dielectric layer.^{10b,13,15} The semiconducting layer was deposited by spin-coating polymer solutions (6 mg/mL in DCB) on untreated Au (Source-Drain)/ SiO_2/Si substrate. After thermal annealing the film at optimized temperature (180 °C) for 10 min, a CYTOP solution was spin-coated on top of the polymer film as the dielectric layer, and an aluminum layer was thermally evaporated as the gate electrode (Figure 3a). We fabricated the devices both in glovebox and in ambient ($R_{\text{H}} = 50\text{--}60\%$) to compare their device performance. All devices were tested in ambient on a probe station. FET devices based on PFI2T fabricated in glovebox and in ambient clearly showed ambipolar transport

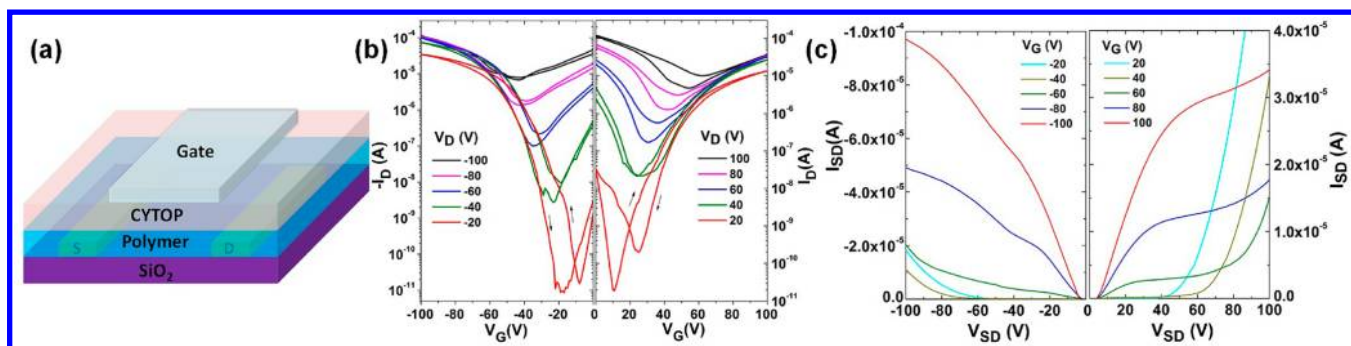


Figure 3. (a) Schematic diagram of TG/BC OFET device structure. (b) The transfer and (c) output characteristics of PFII2T devices fabricated in ambient. OFET devices ($L = 50 \mu\text{m}$, $W = 1000 \mu\text{m}$) were fabricated with CYTOP around 500 nm thick (capacitance $C_i = 3.7 \text{ nF cm}^{-2}$).

Table 1. Summary of Molecular Weight, OFET Device Performance, and GIXD Results of Both Polymers

polymers	M_n (kDa)	PDI	μ_{hole} ($\text{cm}^2 \text{V}^{-1} \text{s}^{-1}$) ^a	V_T (V)	$\log(I_{\text{on}}/I_{\text{off}})$ ^b	μ_{electron} ($\text{cm}^2 \text{V}^{-1} \text{s}^{-1}$) ^a	V_T (V)	$\log(I_{\text{on}}/I_{\text{off}})$ ^c	d (\AA) ^d	
									L	π
PFII2T	75.7	2.58	1.25 (1.13) ^e	-40	5-6	0.51 (0.49) ^e	+32	5-6	29.0	3.55
			1.85 (1.41) ^f	-38	6-7	0.43 (0.38) ^f	+30	5-6		
			0.07 (0.06) ^e	-14	5-6	0.01 (0.004) ^f	+36	3-4		
PII2T	72.8	1.95	0.76 (0.66) ^e	-35	6-7	0.07 (0.06) ^e	+25	5-6	28.8	3.56
			1.27 (1.44) ^f	-14	5-6	0.01 (0.004) ^f	+36	3-4		

^aMeasured in ambient conditions ($R_H = 50-60\%$). Maximum values of hole or electron mobilities and the average values are in parentheses (over 50 devices). ^bEvaluated at $V_D = -20 \text{ V}$. ^cEvaluated at $V_D = +20 \text{ V}$. ^dLamellar (L) and $\pi-\pi$ stacking (π) distances determined by GIXD experiments. ^eDevices fabricated in glovebox. ^fDevice fabricated in ambient conditions.

characteristics. For devices fabricated in glovebox, hole mobilities up to $1.25 \text{ cm}^2 \text{V}^{-1} \text{s}^{-1}$ and electron mobilities up to $0.51 \text{ cm}^2 \text{V}^{-1} \text{s}^{-1}$ were observed (Table 1), which is comparable to several high-performance DPP based polymer FETs.^{2,4}

In addition, all devices fabricated in ambient also exhibit ambipolar properties. The hole mobility is further improved to $1.85 \text{ cm}^2 \text{V}^{-1} \text{s}^{-1}$ with a little decrease in electron mobility. The highest electron mobility is up to $0.43 \text{ cm}^2 \text{V}^{-1} \text{s}^{-1}$, and the average mobility is $0.38 \text{ cm}^2 \text{V}^{-1} \text{s}^{-1}$ (Figure 3). These mobilities are the highest reported to date for an ambipolar FETs fabricated in ambient.¹³ The reference nonfluorinated polymer PII2T shows comparable hole mobilities but decreased electron mobilities. Electron mobilities up to $0.07 \text{ cm}^2 \text{V}^{-1} \text{s}^{-1}$ are observed for devices fabricated in glovebox, but decreased sharply to $10^{-3}-10^{-2} \text{ cm}^2 \text{V}^{-1} \text{s}^{-1}$ for devices fabricated in ambient. Hence, fluorination can substantially increase the ambient stability of the device.

The thin film microstructures and morphologies of both polymers were investigated by grazing incident X-ray diffraction (GIXD) and tapping-mode atomic force microscopy (AFM). In the 2D-GIXD, both polymers appear to have dual textures in thin films (Figure 4a,b). Films of both polymers display strong lamellar textures with five out-of-plane (Q_z) peaks as denoted by ($h00$) Bragg diffraction. The (010) diffraction corresponding to the $\pi-\pi$ stacking distances is observed in both out-of-plane (Q_z) and in-plane (Q_{xy}) diffraction. These results indicate that the polymers have both edge-on and face-on packings in thin films.¹⁶ The measured lamellar and π -stacking distances are almost the same for both polymers (Table 1) because of their similar backbones and identical alkyl chains. However, the ratios of the observed edge-on to face-on packing in film are significantly different for the two polymers. Fluorinated polymer PFII2T displays much stronger ($h00$) diffraction and weaker out-of-plane (010) diffraction. In addition, the in-plane (200) diffraction is only observed for PII2T. These results suggest that PFII2T tends to form the edge-on packing, whereas PII2T

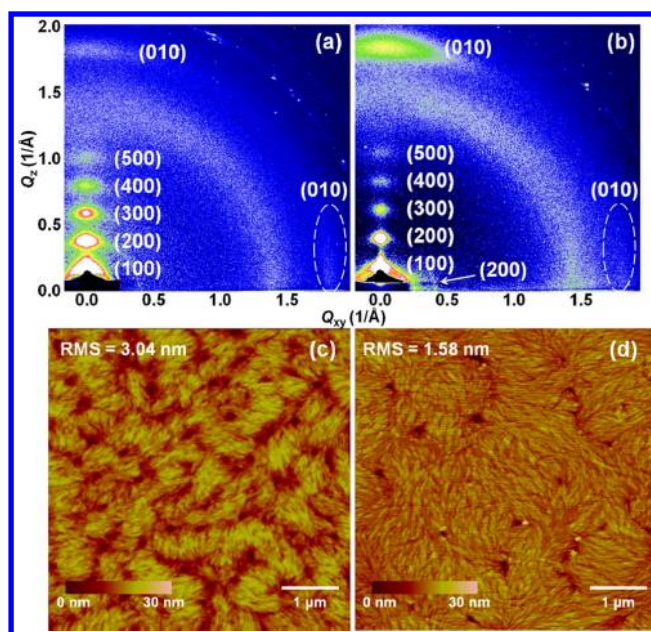


Figure 4. 2D-GIXD patterns of (a) PFII2T and (b) PII2T films. Tapping-mode AFM height images of (c) PFII2T and (d) PII2T films. Films were spin-coated from the DCB solutions of the polymers (6 mg/mL) and annealed at $180 \text{ }^\circ\text{C}$.

tends to form the face-on packing. Scherrer analysis of the (010) diffraction shows that the crystalline coherence length of PFII2T is 62.8 \AA , considerably larger than that of PII2T (43.4 \AA). As illustrated in Figure 4c,d, the AFM images of both polymer films show fibrillar intercalating networks. Crystalline zones similar as other high-performance polymer FET materials¹⁷ are formed, presumably due to strong intermolecular $\pi-\pi$ interactions. In particular, compared with the PII2T film, the PFII2T film has stronger crystalline tendency with larger root-mean-square

(RMS) deviation in the AFM height images, which agrees with the Scherrer analysis. These findings indicate that the introduction of fluorine atoms affects not only energy levels, but also interchain interactions of polymers, creating different polymer packing in films. Since dense molecular packing can result in a barrier to oxygen and water, thereby stabilizing electron transport,¹⁸ we assume that the strong crystallinity and ordered packing in PFII2T may also contribute to its improved ambient stability.

In conclusion, we have demonstrated for the first time that the molecular engineering of the isoindigo core in isoindigo-based donor-acceptor conjugated polymers can dramatically improve the FET performance using these polymers as active layer. Fluorinated isoindigo-based polymer PFII2T shows lowered bandgaps and HOMO/LUMO levels. Ambipolar FETs based on PFII2T can be fabricated and tested in ambient by solution-process, and the electron mobility increases from 10^{-2} to $0.43 \text{ cm}^2 \text{ V}^{-1} \text{ s}^{-1}$ with high hole mobility up to $1.85 \text{ cm}^2 \text{ V}^{-1} \text{ s}^{-1}$. Through fluorination, isoindigo-based polymer PFII2T maintains high hole mobilities, good ambient stability, but above all starts to possess high electron mobilities. GLXD and AFM results also indicate that the introduction of fluorine in electron-deficient isoindigo cores leads to different interchain interactions and stronger crystalline tendency. A combination of the molecular engineering strategies toward isoindigo core (developed herein), donor units (developed previously by us)^{8a} and side chains (developed previously by Bao et al. and us)⁷ may further improve the performance of organic electronics based on these polymers.

■ ASSOCIATED CONTENT

■ Supporting Information

Experimental details and characterization data. This material is available free of charge via the Internet at <http://pubs.acs.org>.

■ AUTHOR INFORMATION

Corresponding Author

jianpei@pku.edu.cn; pxylcj@126.com

Notes

The authors declare no competing financial interest.

■ ACKNOWLEDGMENTS

This work was supported by the Major State Basic Research Development Program (Nos. 2009CB623601 and 2013CB933501) from the Ministry of Science and Technology, and National Natural Science Foundation of China. The authors thank beamline BL14B1 (Shanghai Synchrotron Radiation Facility) for providing the beam time.

■ REFERENCES

- (1) (a) Zaumseil, J.; Sirringhaus, H. *Chem. Rev.* **2007**, *107*, 1296. (b) Beaujuge, P. M.; Fréchet, J. M. J. *J. Am. Chem. Soc.* **2011**, *133*, 20009. (c) Guo, Y.; Yu, G.; Liu, Y. *Adv. Mater.* **2010**, *22*, 4427.
- (2) (a) Zaumseil, J.; Friend, R. H.; Sirringhaus, H. *Nat. Mater.* **2006**, *5*, 69. (b) Bürgi, L.; Turbiez, M.; Pfeiffer, R.; Bienewald, F.; Kirner, H.-J.; Winnewisser, C. *Adv. Mater.* **2008**, *20*, 2217. (c) Huang, H.; Chen, Z.; Ortiz, R. P.; Newman, C.; Usta, H.; Lou, S.; Youn, J.; Noh, Y.-Y.; K., J.; Chen, L. X.; Facchetti, A.; Marks, T. N. *J. Am. Chem. Soc.* **2012**, *134*, 10966.
- (3) (a) Chen, Z.; Lee, M. J.; Ashraf, R. S.; Gu, Y.; Albert-Seifried, S.; Nielsen, M. M.; Schroeder, B.; Anthopoulos, T. D.; Heeney, M.; McCulloch, I.; Sirringhaus, H. *Adv. Mater.* **2012**, *24*, 647. (b) Krone-meijer, A. J.; Gili, E.; Shahid, M.; Rivnay, J.; Salleo, A.; Heeney, M.; Sirringhaus, H. *Adv. Mater.* **2012**, *24*, 1558.

- (4) (a) Yuen, J. D.; Fan, J.; Seifert, J.; Lim, B.; Hufschmid, R.; Heeger, A. J.; Wudl, F. *J. Am. Chem. Soc.* **2011**, *133*, 20799. (b) Bijleveld, J. C.; Zoombelt, A. P.; Mathijssen, S. G. J.; Wienk, M. M.; Turbiez, M.; de Leeuw, D. M.; Janssen, R. A. J. *J. Am. Chem. Soc.* **2009**, *131*, 16616. (c) Nielsen, C. B.; Turbiez, M.; McCulloch, I. *Adv. Mater.* **2012**, DOI: 10.1002/adma.201201795. (d) Shahid, M.; McCarthy-Ward, T.; Labram, J.; Rossbauer, S.; Domingo, E. B.; Watkins, S. E.; Stingelin, N.; Anthopoulos, T. D.; Heeney, M. *Chem. Sci.* **2012**, *3*, 181.
- (5) (a) Pietro, R. D.; Fazzi, D.; Kehoe, T. B.; Sirringhaus, H. *J. Am. Chem. Soc.* **2012**, *134*, 14877. (b) Nicolai, H. T.; Kuik, M.; Wetzelaer, G. A. H.; de Boer, B.; Campbell, C.; Risko, C.; Brédas, J. L.; Blom, P. W. M. *Nat. Mater.* **2012**, *11*, 882.
- (6) (a) Wang, E.; Ma, Z.; Zhang, Z.; Vandewal, K.; Henriksson, P.; Inganäs, O.; Zhang, F.; Andersson, M. R. *J. Am. Chem. Soc.* **2011**, *133*, 14244. (b) Ma, Z.; Wang, E.; Jarvid, M. E.; Henriksson, P.; Inganäs, O.; Zhang, F.; Andersson, M. R. *J. Mater. Chem.* **2012**, *22*, 2306. (c) Wang, E.; Ma, Z.; Zhang, Z.; Henriksson, P.; Inganäs, O.; Zhang, F.; Andersson, M. R. *Chem. Commun.* **2011**, *47*, 4908. (d) Stalder, R.; Mei, J.; Reynolds, J. R. *Macromolecules* **2010**, *43*, 8348. (e) Mei, J.; Graham, K. R.; Stalder, R.; Reynolds, J. R. *Org. Lett.* **2010**, *12*, 660.
- (7) (a) Lei, T.; Dou, J.-H.; Pei, J. *Adv. Mater.* **2012**, DOI: 10.1002/adma.201202689. (b) Mei, J.; Kim, D. H.; Ayzner, A. L.; Toney, M. F.; Bao, Z. *J. Am. Chem. Soc.* **2011**, *133*, 20130.
- (8) (a) Lei, T.; Cao, Y.; Zhou, X.; Peng, Y.; Bian, J.; Pei, J. *Chem. Mater.* **2012**, *24*, 1762. (b) Lei, T.; Cao, Y.; Fan, Y.; Liu, C.-J.; Yuan, S.-C.; Pei, J. *J. Am. Chem. Soc.* **2011**, *133*, 6099.
- (9) Stalder, R.; Mei, J.; Subbiah, J.; Grand, C.; Estrada, L. A.; So, F.; Reynolds, J. R. *Macromolecules* **2011**, *44*, 6303.
- (10) (a) Chen, Z.; Zheng, Y.; Yan, H.; Facchetti, A. *J. Am. Chem. Soc.* **2009**, *131*, 8. (b) Yan, H.; Chen, Z.; Zheng, Y.; Newman, C.; Quinn, J. R.; Doltz, F.; Kestler, M.; Facchetti, A. *Nature* **2009**, *457*, 679. (c) Babel, A.; Jenekhe, S. A. *J. Am. Chem. Soc.* **2003**, *125*, 13656.
- (11) (a) Zhou, E.; Cong, J.; Wei, Q.; Tajima, K.; Yang, C.; Hashimoto, K. *Angew. Chem., Int. Ed.* **2011**, *50*, 2799. (b) Zhan, X. W.; Tan, Z. A.; Domercq, B.; An, Z. S.; Zhang, X.; Barlow, S.; Li, Y. F.; Zhu, D. B.; Kippelen, B.; Marder, S. R. *J. Am. Chem. Soc.* **2007**, *129*, 7246. (c) Chen, J.; Cao, Y. *Acc. Chem. Res.* **2009**, *42*, 1709.
- (12) (a) Chen, H.-Y.; Hou, J.; Zhang, S.; Liang, Y.; Yang, G.; Yang, Y.; Yu, L.; Wu, Y.; Li, G. *Nat. Photonics* **2009**, *3*, 649. (b) Liang, Y.; Feng, D.; Wu, Y.; Tsai, S.-T.; Li, G.; Ray, C.; Yu, L. *J. Am. Chem. Soc.* **2009**, *131*, 7792. (c) Zhou, H.; Yang, L.; Stuart, A. C.; Price, S. C.; Liu, S.; You, W. *Angew. Chem., Int. Ed.* **2011**, *50*, 2995. (d) Price, S. C.; Stuart, A. C.; Yang, L.; Zhou, H.; You, W. *J. Am. Chem. Soc.* **2011**, *133*, 4625.
- (13) Usta, H.; Newman, C.; Chen, Z.; Facchetti, A. *Adv. Mater.* **2012**, *24*, 3678.
- (14) (a) Bondi, A. *J. Phys. Chem.* **1964**, *68*, 441. (b) Rowland, R. S.; Taylor, R. *J. Phys. Chem.* **1996**, *100*, 7384.
- (15) Gamota, D.; Brazis, P.; Kalyanasundaram, K.; Zhang, J. *Printed Organic and Molecular Electronics*; Kluwer Academic Publishers: New York, 2004.
- (16) Wen, Y.; Liu, Y.; Guo, Y.; Yu, G.; Hu, W. *Chem. Rev.* **2011**, *111*, 3358.
- (17) (a) Chen, H.; Guo, Y.; Yu, G.; Zhao, Y.; Zhang, J.; Gao, D.; Liu, H.; Liu, Y. *Adv. Mater.* **2012**, *24*, 4618. (b) Ko, S.; Verploegen, E.; Hong, S.; Mondal, R.; Hoke, E. T.; Toney, M. F.; McGehee, M. D.; Bao, Z. *J. Am. Chem. Soc.* **2011**, *133*, 16722. (c) Osaka, I.; Shimawaki, M.; Mori, H.; Doi, I.; Miyazaki, E.; Koganezawa, T.; Takimiya, K. *J. Am. Chem. Soc.* **2012**, *134*, 3498. (d) Ha, J. S.; Kim, K. H.; Choi, D. H. *J. Am. Chem. Soc.* **2011**, *133*, 10364. (e) Bronstein, H.; Chen, Z.; Ashraf, R. S.; Zhang, W.; Du, J.; Durrant, J. R.; Tuladhar, P. S.; Song, K.; Watkins, S. E.; Geerts, Y.; Wienk, M. M.; Janssen, R. A. J.; Anthopoulos, T.; Sirringhaus, H.; Heeney, M.; McCulloch, I. *J. Am. Chem. Soc.* **2011**, *133*, 3272. (f) Li, Y.; Sonar, P.; Singh, S. P.; Soh, M. S.; van Meurs, M.; Tan, J. *J. Am. Chem. Soc.* **2011**, *133*, 2198.
- (18) Katz, H. E.; Lovinger, A. J.; Johnson, J.; Kloc, C.; Siegrist, T.; Li, W.; Lin, Y. Y.; Dodabalapur, A. *Nature* **2000**, *404*, 478.